ARTICLE

OBC
www.rsc.org/obc

Theozyme for antibody aldolases. Characterization of the transition-state analogue †

Manuel Arnó and Luis R. Domingo *
Instituto de Ciencia Molecular, Departamento de Química Orgánica, Universidad de Valencia, Dr. Moliner 50, E-46100 Burjassot, Valencia, Spain. E-mail: domingo@utopia.uv.es

Received 28th October 2002, Accepted 26th November 2002
First published as an Advance Article on the web 27th January 2003

A theozyme for antibody aldolases has been studied at the MP2/6-31G** computational level. Formation of two cooperative hydrogen-bonds between the acidic hydrogen atoms of the enamine and of a methanol molecule with the oxygen atom of the aldol acceptor markedly favors the C–C bond-formation associated with the aldol reaction. A comparative analysis of the geometry, the charge distribution and the shape of the molecular electrostatic potential of the transition structure (TS) with the covalent adduct, resulting from the reaction of methylamine and the β-diketone used as a hapten allows us to characterize the transition-state analogue (TSA) generated at immunization. This finding allows us to propose a hapten based on a chiral β-ketosulfoxide that could give the formation of a TSA that addresses the tetrahedral geometry of the TS.

Introduction

The aldol reaction is arguably one of the most important C–C bond forming reactions employed in synthetic transformations.[1] As a result of its utility, extensive efforts have been applied to the development of catalytic enantioselective variants of this reaction. Catalytic, enantioselective aldol reactions are typically accomplished with preformed enolates and chiral transition metal catalysts[2] or with natural aldolase enzymes.[3] Two mechanistic classes of aldolase enzymes have evolved.[3b,3c,4,5] Class I aldolases utilize the ε-amino group of a lysine residue (Lys) in the active site to form a Schiff base with one of the substrates, which activates the substrate as an aldol donor, while Class II aldolases are metalloenzymes that facilitate enolate formation by coordination to the substrate's carbonyl oxygen.

For Class I aldolases the reaction is bimolecular and proceeds through several intermediates (see Scheme 1).[4,5] Firstly, an

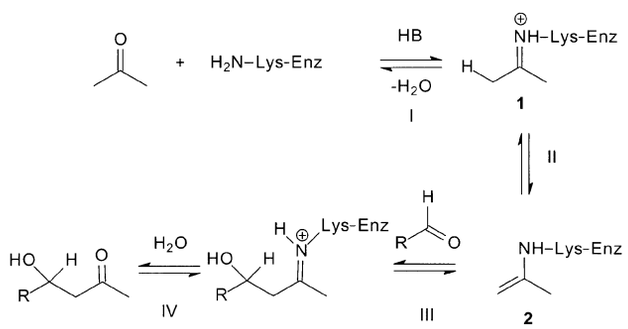

Scheme 1

iminium ion **1**, a Schiff base, is formed (step I) that by a proton abstraction from the α carbon atom gives the corresponding enamine **2** (step II). This acts as nucleophile that reacts with aldehydes or ketones to form a new C–C bond (step III). The new iminium ion is hydrolyzed, and the product is released (step IV). The essence of this mechanism is the formation of the enamine **2**, which is a good aldol donor. The rate and stereochemical-determining step corresponds with the C–C bond-formation in step III.[5]

An approximation to natural enzymes is the antibody catalyst. Transition-state analogues (TSA) are compounds with a fixed shape that resemble the geometry and charge distribution of a given transition structure (TS). In the antibody catalyst, interactions at the binding site similar to those performed with the TSA at immunization can stabilize the TS for the rate-determining step, increasing the rate. However, the construction of TSAs is generally difficult because the geometries of the TSs are inherently unstable owing to their transient nature.

Several studies have been devoted to generating antibodies that use the reaction mechanisms that give aldolases their efficiency but that take advantage of the range of substrates and stereochemical specificities available with antibodies. Thus, the aldolase antibodies ab38C2 (Aldrich no. 47,995–0), ab84G3 (Aldrich no. 52,785–8), and the ab33F12, which can be classified as models of the Class I aldolases, are able to catalyze both the aldol and retro-aldol reactions.[4,6,7] They have an advantage over the natural aldolases as they accept a wide range of substrates.[5,8] These antibodies were raised against the β-diketone hapten **3** which serves as a chemical trap to imprint the lysine-dependent Class I aldolase mechanism on the binding site of the antibody (see Scheme 2). The ε-amino group of the Lys

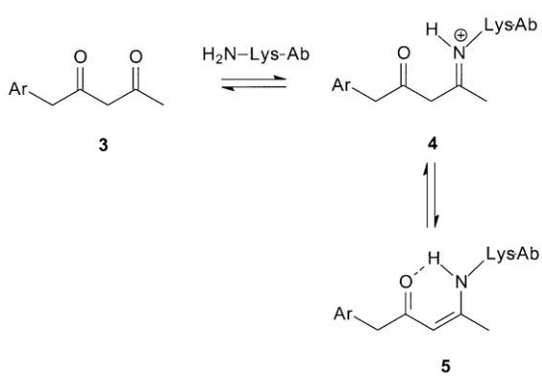

Scheme 2

reacts with a carbonyl group of the β-diketone moiety of **3** to form a β-ketohemiaminal which by a subsequent dehydratation gives the β-ketoimine **4**. Finally, **4** tautomerizes into a more stable enaminone **5** because of the formation of an intramolecular hydrogen-bond. Consequently, the hapten **3** is covalently bound in the binding pocket.[4,5,7] The importance of

† Electronic supplementary information (ESI) available: MP2/6-31G** energies, imaginary frequencies and cartesian coordinates. See http://www.rsc.org/suppdata/ob/b2/b209636f/

DOI: 10.1039/b209636f

LysH93 to the formation of the enamine has been indicated by the crystal structural data of ab33F12 and by mutagenesis experiments.[9,10]

While the antibodies ab38C2 and ab33F12 obtained against the achiral β-diketone hapten **3** catalyze the aldol reaction with a large enantioselectivity resulting from an attack on the carbonyl group along the *Si*-face,[5] the antibodies ab84G3, ab93F3 and ab85H6 obtained against the chiral β-diketosulfone hapten **6** afford aldol products that are antipodal to those prepared with ab38C2 and ab33F12 (see Scheme 3).[6b,11] Furthermore, the

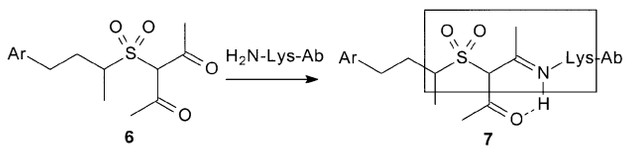

Scheme 3

sulfone **6** also gave antibodies ab40F12 and ab42F1[10] which have the same enantioselectivity as those obtained with hapten **3** but were formed with similar even minor efficiency.[12] The β-diketosulfone **6** was designed because the original hapten **3** does not address the tetrahedral geometry of the TS of the rate-determining C–C bond-formation step.[11]

The C–C bond-formation step for the amine-catalyzed aldol reaction involving enamine intermediates has been recently theoretically studied by Bahmanyar and Houk.[13] The formation of a hydrogen-bond between the hydrogen of the primary amine and the carbonyl oxygen atom of the aldol acceptor favors the C–C bond-formation step through stabilization of the negative charge that is developing at the carbonyl oxygen atom. The B3LYP/6-31G* activation barrier for the process was 14 kcal mol^{-1}. While primary enamines give the aldol adduct directly in a concerted fashion, secondary enamine-mediated aldol reactions give zwitterionic intermediates, since there is no NH or other proton source to transfer to the developing alkoxide.[13]

Houk has defined a *theozyme* as "an array of functional groups in a geometry predicted by theory to provide transition-state stabilization".[14] Such a hypothetical arrangement of functional groups fixed in space by arbitrary constraints, provides a means for the quantitative assessment of the contribution of individual atomic interactions to catalysis. The array of functional groups are supplied by small molecules as methanol and formic acid and/or their conjugated bases, which allows us to model the acid/base residues present at the binding site.[15] The theozymes have been employed to obtain a better understanding of biological catalysts or to design new inhibitors, haptens or synthetic catalysts.[16,17] On the basis of the theozyme definition, we have recently reported two theoretical studies for the design of TSAs for the disfavored intramolecular Michael addition of 6-hydroxy-α,β-unsaturated esters,[17a] and the acid/base catalyzed intramolecular aldol reaction of δ-diketones[17b] in order to design adequate TSAs for the C–C bond-formation step. These studies show that the presence of appropriately positioned acid/base residues in the binding site, which allows a favorable electronic stabilization of the TS, can assist a disfavored chemical reaction. In particular, for the aldol reaction the C–C bond-formation step is markedly favored by an increase of the nucleophilicity of the donor enol, (base catalysis) and an increase in the electrophilicity of the acceptor carbonyl compound (acid catalysis).[17b] Now we present herein the results of a study for a theozyme for C–C bond-formation involving antibody aldolases, capable of explaining the large effectiveness of these antibodies, which is comparable to natural aldolases. In addition, the TSA associated with these antibody aldolases will be characterized. Finally, a new chiral hapten, that could afford the formation of a TSA that addresses the tetrahedral geometry of the TS, is designed.

Computational methods

All calculations were carried out with the Gaussian 98 suite of programs.[18] An exhaustive exploration of the potential energy surfaces (PESs) was carried out at the MP2/6-31G** level.[19] The optimizations were carried out using the Berny analytical gradient optimization method.[20] The stationary points were characterized by frequency calculations in order to verify that minima and TSs have zero and one imaginary frequency, respectively. The intrinsic reaction coordinate (IRC)[21] paths were traced in order to check the energy profiles connecting each TS to the two associated minima of the proposed mechanism by using the second order González–Schlegel integration method.[22] The bond orders (BO)[23] were computed using the natural bond orbital (NBO) method.[24] The reported point charges are based on fitting to the computed electrostatic potential using the CHELPG scheme.[25] Electrostatic potential surfaces were generated using SPARTAN.[26] The electrostatic potential for each structure was mapped onto a total electron density surface contoured at 0.002 e au^{-3}. Cartesian coordinates for all stationary points are given in the supplementary material.

The polarity effects of the binding site on these antibody catalyzed reactions have been investigated by single point calculations at the optimized gas phase geometries using the self-consistent reaction field (SCRF)[27] cavity model with the PCM option.[28] Since it has been proposed that the combining site of ab33F12 is surrounded by mostly hydrophobic side chains,[9] it being similar to that given by the *n*-octanol medium[5b] ($\varepsilon = 10.3$), we have chosen the relative permittivity value of $\varepsilon = 10.4$ (dichloroethane).

Results and discussion

Firstly, a brief discussion of the C–C bond-formation step for the primary-amine catalyzed aldol reaction will be presented. Then, a theozyme explaining the effectiveness of the aldolase antibodies will be discussed. Finally, the structure of the TSAs generated at immunization will be analyzed. A new chiral hapten that could address the formation of a TSA that would mimic the tetrahedral arrangement of the TS is designed.

a) Study of the C–C bond-formation step on the primary-amine catalyzed aldol reaction.

Both Class I aldolases and antibody aldolases use enamines generated from primary amines to activate the methylene group of the donor carbonyl compound for the C–C bond-formation step. Thus the nucleophilic attack of the enamine **9** on acetaldehyde **8** was firstly studied (see Scheme 4). This step has been recently studied by Bahmanyar and Houk in the study of the mechanism of the amine catalyzed aldol reactions involving enamine intermediates.[13] For this step two reactive channels are feasible. They are related to the *syn* and *anti* arrangement of the enamine hydrogen atom relative to the active methylene group. Therefore, two TSs, **TS-1** and **TS-2**, and their corresponding adducts **10** and **11**, associated with the *syn* and *anti* reactive channels respectively, have been studied. The geometries of the TSs are shown in Fig. 1, while the relative energies are given in Table 1.

An analysis of the IRC from TSs to reactants allows us to find two molecular complexes (MC), **MC-1** and **MC-2**, associated with an early stage of the C–C bond-formation process (see Scheme 4). Both MCs are 5.6 and 6.5 kcal mol^{-1}, respectively, more stable that the separated reactants due to the formation of an intermolecular hydrogen-bond between the amine hydrogen atom and the oxygen atom of the carbonyl acceptor.

The MP2/6-31G** barriers for the C–C bond-formation process, *via* **TS-1** and **TS-2**, relative to the MCs are 13.8 and 33.7 kcal mol^{-1}, respectively. Therefore, the formation of the

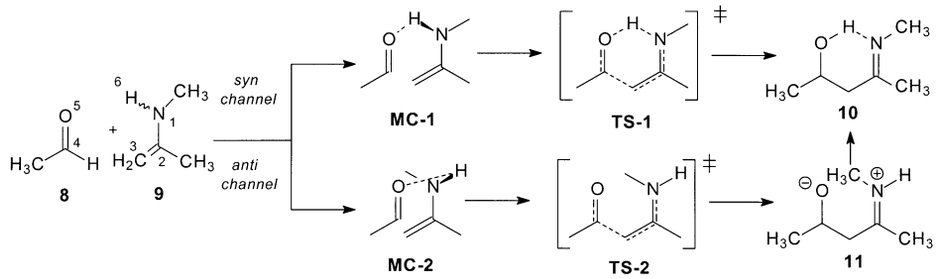

Scheme 4

Table 1 Total energies (au) and relative energies[a,b] (kcal mol^{-1}, in parentheses) of the stationary points for the reaction between **8** and **9** in the absence and presence of a methanol molecule

	MP2/6-31G**		MP2/6-31G** SCF// MP2/6-31G** (ε = 10.36)	
8	−153.378467		−153.380436	
9	−211.881682		−211.883742	
12	−268.773900		−268.774712	
MC-1	−365.269131		−365.268587	
MC-2	−365.273754		−365.272143	
MC-3	−480.662425		−480.661036	
TS-1	−365.245544	(13.8)	−365.250830	(10.1)
TS-2	−365.220508	(33.7)	−365.236593	(22.6)
TS-3	−480.644043	(11.1)	−480.648201	(7.7)
10	−365.300848	(−18.6)	−365.305394	(−21.8)
11	−365.218915	(35.1)	−365.238326	(21.9)
13	−480.698989	(−20.9)	−480.702369	(−23.9)

[a] Relative to the corresponding molecular complex. [b] Relative energies including zero point vibrational energies and thermochemical corrections to enthalpies at 25 °C.

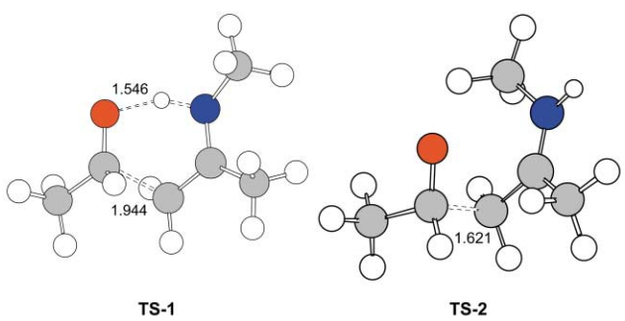

Fig. 1 Transition structures corresponding to the C–C bond-formation step for the primary-amine catalyzed aldol reaction.

hydrogen-bond at **TS-1** favors the C–C bond-formation step. These barriers are similar to those found by Bahmanyar and Houk at the B3LYP/6-31G* level.[13] The *syn* channel is thermodynamically favored because of the formation of the neutral iminol **10**; the process is exothermic by −18.6 kcal mol^{-1}. However, the zwitterionic character of the intermediate **11** makes the *anti* channel strongly endothermic, 35.1 kcal mol^{-1}. Inclusion of environmental effects using a SCRF method stabilizes the TSs and adducts between 3–10 kcal mol^{-1} because of the large polar character of these species. The **TS-2** and intermediate **11** are strongly stabilized because of their zwitterionic nature. Nevertheless the *syn* channel remains more favorable than the *anti* one; the barrier for **TS-1** (10.1 kcal mol^{-1}) is 12.6 kcal mol^{-1} less energetic than that for **TS-2**.

The lengths of the C3–C4 forming bond at **TS-1** and **TS-2** are 1.944 and 1.621 Å, respectively. The N1–H6 and O5–H6 bond lengths at **TS-1** are 1.073 and 1.546 Å, respectively. The BO values of the C3–C4 forming bond are 0.52 (**TS-1**) and 0.85 (**TS-2**). The BO values of the N1–H6 and O5–H6 bonds at **TS-1** are 0.59 and 0.13, respectively. If we consider that the N1–H6 BO value at this TS is slightly lower than that at the corresponding molecular complex **MC-1**, these BO values indicate that the proton transfer at **TS-1** is more delayed than the C–C bond-formation process.[17b]

b) Study of a theozyme for antibody aldolases.

The large efficacy of natural enzymes is attributed mainly to the feasibility of simultaneous acid/base interactions of the TS with key residues present at the binding site, which allow electronic stabilization of the corresponding TS. This efficacy is not feasible in a homogeneous reaction medium because of the inherent nature of the acid/base catalysts. The X-rays of Class I and antibody aldolases show the presence of -OH hydroxy groups belonging to tyrosine (Tyr), threonine (Thr) and glutamic acid at the binding site,[5,9,10] which can act as proton donors in acid catalysis. Thus, an analysis of the binding site of Fab' ab33F12[9,29] shows that LysH93 is surrounded by three tyrosine residues, TyrH95, TyrL36 and TyrL96, and one threonine residue, ThrL97. A view of the Fab' ab33F12 binding site showing these acidic residues within the vicinity of LysH93 is shown in Fig. 2. In this illustration, the L and H chains are

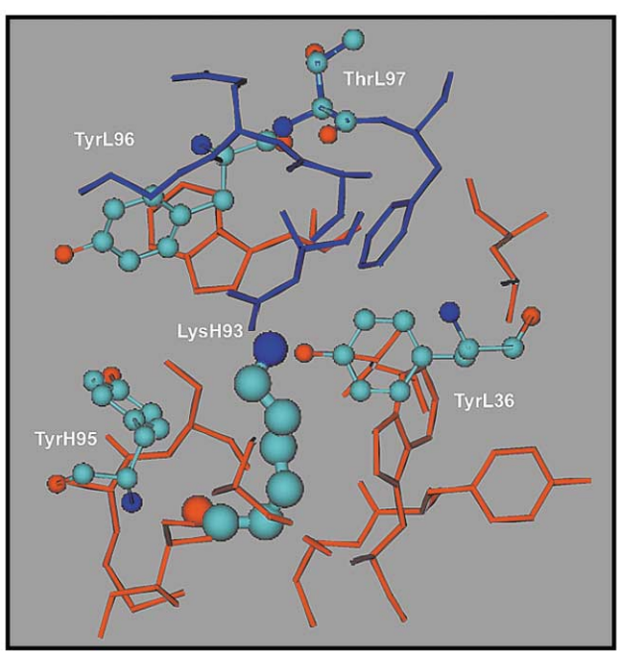

Fig. 2 A view of the Fab' ab33F12 binding site showing the acidic residues (<7 Å) within the vicinity of LysH93.

represented in blue and red respectively, while the tyrosine and threonine residues are in atom colours. An analysis of the distances between the oxygen atoms bound to the acidic hydrogen atoms of these key residues and the primary-amine nitrogen atom of the LysH93 shows that they are in the narrow range of 5–7 Å. Therefore, these acid residues can interact with the basic region of **MC-1** and **TS-1** that corresponds with the O5 oxygen atom of the carbonyl acceptor (see later).

In order to investigate the feasibility of the formation of a second hydrogen-bond at **MC-1**, two MCs in which acetaldehyde is hydrogen-bonded to one or two methanol molecules was studied. An analysis of the MP2/6-31G** energetic results indicates that while the formation of the first hydrogen-bond is thermodynamically favored by 5.2 kcal mol^{-1}, the formation of the second hydrogen-bond becomes more favorable. The stabilization with the formation of two hydrogen-bonds is 15.8 kcal mol^{-1}.

Consequently, a theozyme in which a methanol molecule was hydrogen-bonded to the basic oxygen atom of the aldol acceptor was studied in order to investigate the effects of an additional hydrogen-bond from a key residue on the C–C bond-formation step (see Scheme 5). Thus, a MC, **MC-3**, a TS, **TS-3**, and an adduct, **13**, have been studied (see Scheme 6). The geom-

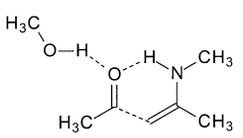

Theozyme for the antibody aldolases

Scheme 5

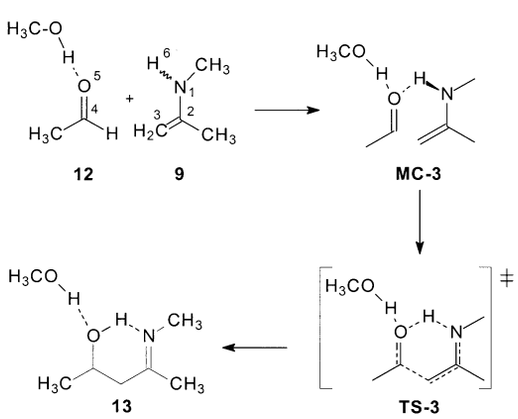

Scheme 6

etry of these species are shown in Fig. 3, while the relative energies are given in Table 1. In Fig. 4 the energy profiles for the C–C bond-formation step for the primary-amine catalyzed reaction in the absence (**MC-1**, **TS-1** and **10**) and in the presence of a methanol molecule (**MC-3**, **TS-3** and **13**) are shown.

The formation of **MC-3** is thermodynamically favorable; **MC-3** is 7.5 kcal mol^{-1} lower in energy than **MC-2** plus methanol. The barrier for the methanol catalyzed process *via* **TS-3** (11.1 kcal mol^{-1}) is 2.7 kcal mol^{-1} lower in energy than that for **TS-1**. Therefore, the presence of the intermolecular hydrogen-bond to the oxygen atom of the aldol acceptor has an additional favorable effect on the reduction of the activation energy. Inclusion of environmental effects decreases the barrier *ca.* 3.4 kcal mol^{-1} relative to that obtained in the gas phase. These energetic results indicate that in the binding site the simultaneous formation of two hydrogen-bonds at the carbonyl aldol acceptor markedly favors the C–C bond-formation process though a larger reduction of the activation energy, explaining the effectiveness of the antibody aldolases (see Fig. 4).[3]

The barrier found for the C–C bond-formation step *via* **TS-3**, 7.7 kcal mol^{-1}, is similar to that found for the proline-catalyzed aldol reaction,[30] which constitutes a bioorganic approach to the aldolases (the B3LYP/6-31G** barrier for the C–C bond-formation step for the proline-catalyzed process in DMSO is 7.0 kcal mol^{-1}). On the binding site the barrier can be even lower than that obtained for **TS-3** because of the more acidic character of the phenolic –OH of tyrosine than methanol.[30c]

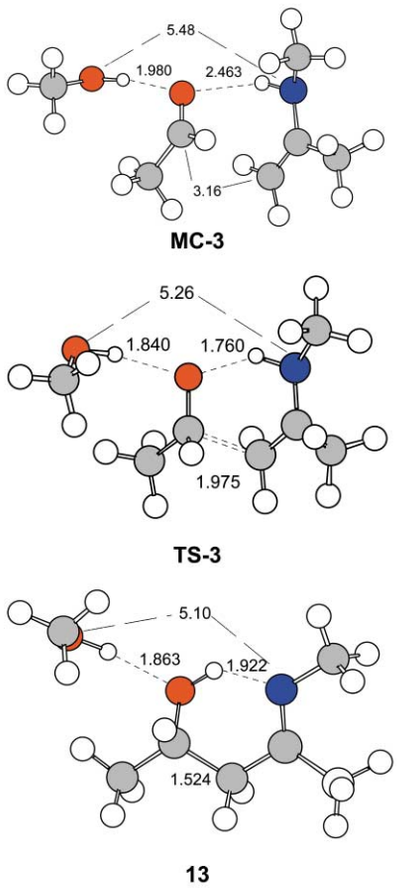

Fig. 3 Molecular complex, **MC-3**, transition structure, **TS-3**, and aldol adduct, **13**, associated with the C–C bond-formation process at the theozyme for the antibody aldolases.

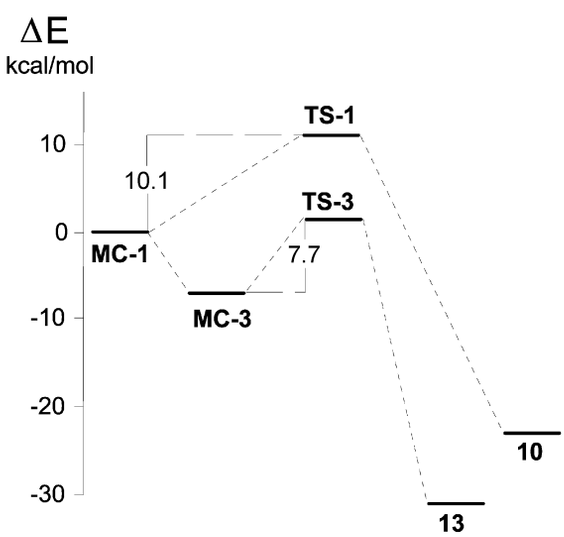

Fig. 4 B3LYP/6-31G** (SCF, ε = 10.36) energy profiles for the C–C bond-formation step for the primary-amine catalyzed reaction in the absence, (**MC-1**, **TS-1** and **10**) and in the presence of a methanol molecule (**MC-3**, **TS-3** and **13**).

The length of the C3–C4 forming bond at **TS-3** is 1.975 Å, similar to that found for **TS-1**. A comparison between the geometries of the *syn* TSs in the absence and in the presence of methanol, **TS-1** and **TS-3**, shows that there are no significant differences (see Figs. 1 and 3). The lengths of the two hydrogen-bonds of **TS-3** are 1.840 and 1.760 Å. The distance between the oxygen atom of methanol and the nitrogen atom of the enamine of **TS-3**, *ca.* 5.3 Å, is within the range of the distances found between the oxygen atoms of the key residues and

the nitrogen atom of the LysH93, 5–7 Å, at the binding site of ab33F12.

The BO value of the C3–C4 forming bond at **TS-3** is 0.49, while the BO values between the O5 oxygen atom and the acidic hydrogen atoms of methanol and the enamine are 0.04 and 0.06, respectively. Both bond lengths and BO values indicate that these acidic hydrogen atoms are not being transferred to the TS. Thus, an analysis of the IRC from **TS-3** to adduct **13** shows that the amine hydrogen atom is transferred to the carbonyl oxygen atom after the formation of the C–C bond in an unbroken fashion to give the neutral imine-alcohol **13**, without the participation of any zwitterionic intermediate. In addition, the methanol molecule remains hydrogen-bonded to the carbonyl oxygen atom during the C–C bond-formation process.

c) Characterization of the TSA associated with the antibody aldolases.

An analysis of the geometry of the covalent structure **5** raised against the β-diketones **3** used as hapten at immunization shows that it resembles the *syn* transition structures **TS-1** and **TS-3** (see Schemes 2 and 4). Therefore, covalent structures such as **5** are TSAs for the antibody aldolases. In order to corroborate this assertion, a study of the geometrical and electronic similarity[31] between **TS-1** and the covalent structure obtained from the reaction between methylamine and the β-diketone **14** (**TSA-1**), as a model of the covalent adduct **5** generated at immunization, was performed (see Scheme 7). The geometry of **TSA-1** is presented in Fig. 5.

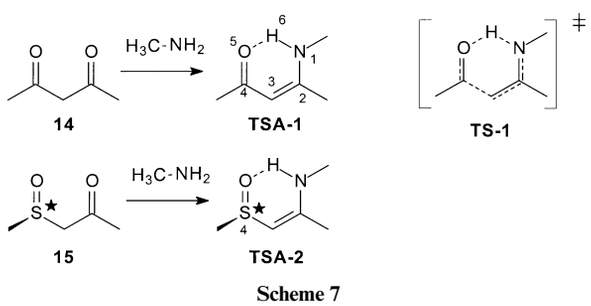

Scheme 7

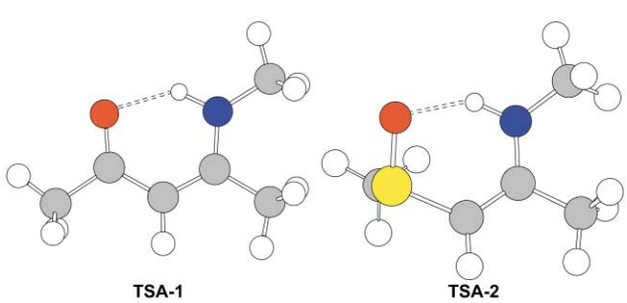

Fig. 5 Transition structure analogues obtained from the reaction of methylamine with the β-diketone **14** and with the β-ketosulfoxide **15**.

The shapes of **TS-1** and **TSA-1** have been compared by means of a geometrical analysis between the position of the heavy atoms (not including hydrogen atoms) of **TS-1** and **TSA-1** using the option COMPARE of the PCMODEL program.[32] The geometrical similarity has been evaluated by examining the root mean square (rms) of the atomic positions.[17] An analysis of the results given in Table 2 shows that **TSA-1** presents a low rms value, 0.472, indicating that it is geometrically very similar to **TS-1**. In addition, if we compare only the atoms involved in the reaction (N1, C2, C3, C4 and O5) this value decreases to 0.273. This result agrees with the fact that the N1–O5 distances, which provide a measure of the relative position of the basic O5 oxygen atom relative to the Lys N1 nitrogen atom, are very similar: 2.48 Å at **TS-1** and 2.65 Å at **TSA-1**. Finally, the molecular volume for **TS-1** and **TSA-1**, which is indicative of the space occupied at the binding site, is also very similar (see Table 2).

Table 2 CHELPG charges[a] (au) and electrostatic potentials (kcal mol^{-1}) for selected atoms, rms (atoms involved in the reaction in parenthesis) for TSAs with respect to **TS-1**, molecular volumes, and N1–O5 distances (angstroms)

	TS-1	TSA-1	TSA-2
CHELPG charges			
O5	−0.81	−0.72	−0.57
X4	0.76	0.85	0.32
C3	−0.80	−0.93	−0.44
C2	0.71	0.64	0.51
N1	−0.72	−0.60	−0.53
H1	0.47	0.42	0.39
Electrostatic potentials			
O5	−62.6	−54.1	−59.9
H1	8.5	20.0	14.6
Rms		0.472 (0.273)	0.706 (0.329)
Volumes (A^3)	157.7	150.6	159.5
N1–O5 Distances	2.480	2.654	2.772

[a] X = C (**TSA-1**) or S (**TSA-2**).

The electronic similarity between **TS-1** and **TSA-1**, which is an indication that the antibody can recognize the TS, has been estimated by comparing the charge distribution[17,33] and the molecular electrostatic potential[15,17,33,34] (MEP) of **TS-1** and **TSA-1**. Analysis of the CHELPG charges for **TS-1** shows a high negative charge at the O5 oxygen atom, −0.8 au, which corresponds with the basic center that will be hydrogen-bonded to the acidic hydrogen atom of a key residue. For **TSA-1**, the negative charge located on the O5 basic center, −0.7 au, is very similar to that found at **TS-1**. A comparison of the charges at the N1, C3, C4 and H6 atoms of **TS-1** and **TSA-1** shows a large electronic similarity between these species. The C3 carbon atom of **TSA-1** that would simulate the methylene of the enamine of **TS-1** also presents a large negative charge, −0.9 au. Finally, we carried out an MEP analysis to compare **TS-1** and **TSA-1** (see Fig. 6). In these species, the largest concentration of negative

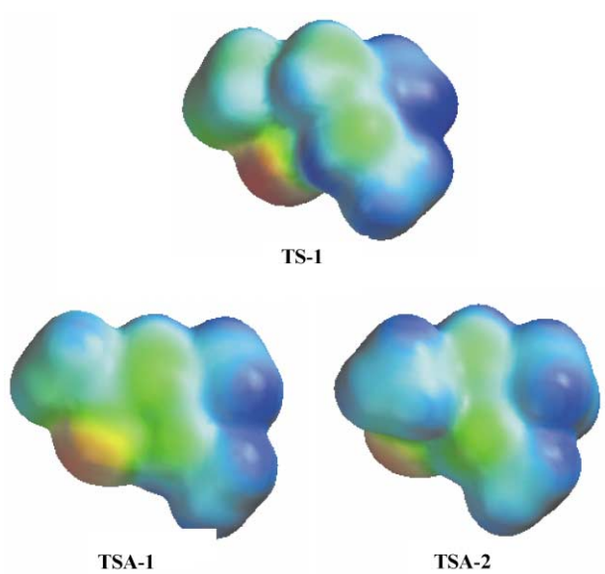

Fig. 6 Electrostatic potential surface for **TS-1** and TSAs **TSA-1** and **TSA-2** graphed over the range of −58–28 kcal mol^{-1}. The red area corresponds to the region where the electrostatic potential is most negative (O5), and blue is associated with the positive region (CH_3).

charge (red region) is found around the O5 oxygen atom. Thus, at both **TS-1** and **TSA-1** the negatively charged O5 oxygen atom corresponds with the basic center that will be hydrogen-bonded to an acid residue.[17] The potential energy ranges were −65–32 kcal mol^{-1} for **TS-1** and −54–26 kcal mol^{-1} for **TSA-1**. Thus, the TSA presents similar ranges to those for **TS-1**. As can be observed, the shape and the volume of the MEP of this TSA closely resembles that of **TS-1** (see Fig. 6). Therefore, the TSA is able to duplicate the electrostatic interactions of **TS-1** at the binding site.

Both **TS-1** and **TSA-1** have the main frameworks, enamine or iminium and carbonyl groups, in a similar arrangement, and with the amine hydrogen atom in a *syn* arrangement relative to the carbonyl group. Thus, we can assert that **TSA-1** corresponds to the covalent TSA generated at immunization. Note that at both **TS-1** and **TSA-1** the O5 oxygen atoms, which can induce formation of the second hydrogen-bond, present a large negative charge in spite of the presence of the intramolecular hydrogen-bond. This large similitude allows us to explain the high efficiency catalyst induced at the corresponding aldolase antibody that is comparable to natural enzymes.[3]

Finally, we present herein the chiral β-ketosulfoxides **15** as an alternative model for the achiral β-diketosulfone hapten **6** (see Schemes 7 and 8), since the pyramidal arrangement around the

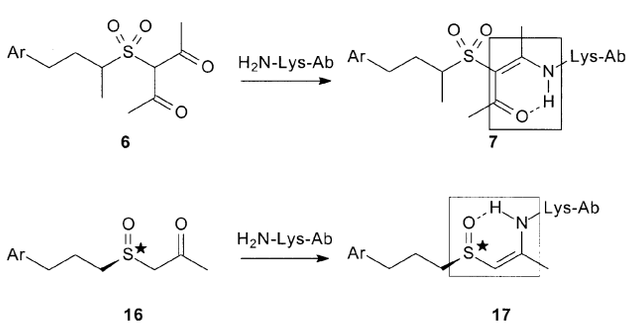

Scheme 8

chiral S4 sulfur atom would mimic the tetrahedral TS. The haptens containing the β-ketosulfoxide framework could be capable of generating antibodies which give double enantioselectivity through formation of chiral TSAs such as **TSA-2**.[12] Thus, a comparative analysis of the geometrical and electronic similarity between **TS-1** and **TSA-2** (see Table 2 and Fig. 6) shows that the latter has a similar shape and charge distribution to those found for **TS-1** and **TSA-1**. In addition, the chirality imposed by the sulfoxide group present in **16**, in contrast to the achiral diketosulfone **6** will facilitate enantioselectivity (see the TSA **7** raised against the β-diketosulfone hapten **6**, and the proposed TSA **17** in Scheme 8). Note, the framework corresponding to the core of the TSA **17** compared with that proposed in previous works (Scheme 3).

Conclusions

A theozyme for antibody aldolases has been studied. Formation of two cooperative hydrogen-bonds between the acidic hydrogen atoms of the enamine, and of a methanol molecule with the oxygen atom of the aldol acceptor, markedly favor the C–C bond-formation associated with the aldol reaction. A comparative analysis of the geometry, the charge distribution and the shape of the molecular electrostatic potential of the TS for the C–C bond-formation process, and the covalent product of the reaction of methylamine and the β-diketone used as a hapten allows us to present herein this covalent adduct as the TSA for the antibody aldolases. The large similarity between these covalent species and the TS of the process explains the effectiveness of these antibodies, which are comparable to natural aldolases. Finally, a chiral β-ketosulfoxide is proposed as an alternative to the β-ketosulfones in order to induce enantioselectivity at the C–C bond-formation step, because the pyramidal arrangement around the chiral sulfur atom can mimic the chirality of the tetrahedral transition structure.

Acknowledgements

This work was supported by research funds provided by the Ministerio de Educación y Cultura of the Spanish Government by DGICYT (projects PB98–1429 and BQU2002–01032). All calculations were performed on a Cray-Silicon Graphics Origin 2000 of the Servicio de Informática de la Universidad de Valencia. We are most indebted to this center for providing us with computer capabilities.

References

1 For reviews of the aldol reaction see: (*a*) S. Masamune, W. Choy, J. S. Petersen and L. R. Sita, *Angew. Chem. Int. Ed. Engl.*, 1985, **24**, 1–30; (*b*) D. A. Evans, *Science*, 1988, **240**, 420–426; (*c*) C. H. Heathcock, *Aldrichimica Acta*, 1990, 99–111; (*d*) A. S. Franklin and I. Paterson, *Contemp. Org. Synth.*, 1994, **1**, 317; (*e*) C. J. Cowden and I. Paterson, *Org. React.*, 1997, **51**, 1.

2 (*a*) E. M. Carreira, W. Lee and R. A. Singer, *J. Am. Chem. Soc.*, 1995, **117**, 3649–3650; (*b*) A. Yanagisawa, Y. Matsumoto, H. Nakashima, K. Asakawa and H. Yamamoto, *J. Am. Chem. Soc.*, 1997, **119**, 9319–9320; (*c*) D. A. Evans, D. W. C. MacMillan and K. R. Campos, *J. Am. Chem. Soc.*, 1997, **119**, 10859–10860; (*d*) S. G. Nelson, *Tetrahedron: Asymmetry*, 1998, **9**, 357–389; (*e*) D. J. Ager and M. B. East, *Asymmetric Synthetic Methodology*, CRC Press, Boca Raton, 1996; (*f*) E. M. Carreira, in *Comprehensive Asymmetric Catalysis*, eds. E. N. Jacobsen, A. Pfaltz and H. Yamamoto, Springer-Verlag, Heidelberg, 1999, Vol III, Chapter 29.1.

3 (*a*) M. D. Bednarski, in *Comprehensive Organic Synthesis*, ed. B. M. Trost, Pergamon, Oxford, 1991, Vol. 2, pp 455–473; (*b*) C. H. Wong and G. M. Whiteside, *Enzymes in Synthetic Organic Chemistry*, Pergamon, Oxford, 1994; (*c*) T. D. Machajewski and C.-H. Wong, *Angew. Chem., Int. Ed.*, 2000, **39**, 1352–1374.

4 J. Wagner, R. A. Lerner and C. F. Barbas III, *Science*, 1995, **270**, 1797–1880.

5 (*a*) J. L. Reymond and Y. Chen, *J. Org. Chem.*, 1996, **60**, 6970–6979; (*b*) T. Hoffmann, G. Zhong, B. List, D. Shabat, J. Anderson, S. Gramatikova, R. A. Lerner and C. F. Barbas III, *J. Am. Chem. Soc.*, 1998, **120**, 2768–2779.

6 (*a*) B. List, D. Shabat, G. Zhong, J. M. Turner, A. Li, T. Bui, J. Anderson, R. A. Lerner and C. F. Barbas III, *J. Am. Chem. Soc.*, 1999, **121**, 7283–7291; (*b*) S. C. Sinha, J. Sun, G. Miller, C. F. Barbas III and R. A. Lerner, *Org. Lett.*, 1999, **1**, 1623–1626.

7 (*a*) F. Tanaka, R. A. Lerner and C. F. Barbas III, *Chem. Commun.*, 1999, 1383–1383; (*b*) F. Tanaka, R. A. Lerner and C. F. Barbas III, *J. Am. Chem. Soc.*, 2000, **122**, 4835–4836.

8 (*a*) G. Zhong, T. Hoffmann, R. A. Lerner, S. Danishefsky and C. F. Barbas III, *J. Am. Chem. Soc.*, 1997, **119**, 8131–8132; (*b*) D. Shabat, B. List, R. A. Lerner and C. F. Barbas III, *Tetrahedron Lett.*, 1999, **40**, 1473–1440; (*c*) B. List, R. A. Lerner and C. F. Barbas III, *Org. Lett.*, 1999, **1**, 59–61.

9 C. F. Barbas III, A. Heine, G. Zhong, T. Hoffmann, S. Gramatikova, R. Björnestedt, B. List, J. Anderson, E. A. Stura, E. A. Wilson and R. A. Lerner, *Science*, 1997, **278**, 2085–2095.

10 A. Karlstrom, G. Zhong, C. Rader, N. A. Larsen, A. Heine, R. Fuller, B. List, F. Tanaka, I. A. Wilson, C. F. Barbas III and R. A. Lerner, *Proc. Natl. Acad. Sci. U. S. A.*, 2000, **97**, 3878–3883.

11 G. Zhong, R. A. Lerner and C. F. Barbas III, *Angew. Chem., Int. Ed.*, 1999, **38**, 3738–3741.

12 A. J. Kirby, *Acta Chem. Scand.*, 1996, **50**, 203–210.

13 S. Bahmanyar and K. N. Houk, *J. Am. Chem. Soc.*, 2001, **123**, 11273–11283.

14 D. J. Tantillo, J. Chen and K. N. Houk, *Curr. Opin. Chem. Biol.*, 1998, **2**, 743–750.

15 (*a*) J. Na, K. N. Houk and D. Hilvert, *J. Am. Chem. Soc.*, 1996, **118**, 6462–6471; (*b*) A. Venturini, F. López-Ortiz, J. M. Alvarez and J. Gonzalez, *J. Am. Chem. Soc.*, 1998, **120**, 1110–1111; (*c*) E. Y. Lau, Z. E. Newby and T. C. Bruice, *J. Am. Chem. Soc.*, 2001, **123**, 3350–3357.

16 (*a*) J. M. Coxon and A. J. Thorpe, *J. Am. Chem. Soc.*, 1999, **121**, 1095–10957; (*b*) M. Oliva, V. S. Safont, J. Andrés and O. Tapia,

J. Phys. Chem. A, 1999, **103**, 8725–8732; (*c*) N. Diaz, D. Suarez and K.M.M. Merz, *J. Am. Chem. Soc.*, 2000, **122**, 4197–4208.
17 (*a*) M. Arnó, L. R. Domingo and J. Andrés, *J. Org. Chem.*, 1999, **64**, 9164–9169; (*b*) M. Arnó and L. R. Domingo, *Int. J. Quantum Chem.*, 2001, **83**, 338–347.
18 M. J. Frisch, G. W. Trucks, H. B. Schlegel, G. E. Scuseria, M. A. Robb, J. R. Cheeseman, V. G. Zakrzewski, J. A. Montgomery, Jr., R. E. Stratmann, J. C. Burant, S. Dapprich, J. M. Millam, A. D. Daniels, K. N. Kudin, M. C. Strain, O. Farkas, J. Tomasi, V. Barone, M. Cossi, R. Cammi, B. Mennucci, C. Pomelli, C. Adamo, S. Clifford, J. Ochterski, G. A. Petersson, P. Y. Ayala, Q. Cui, K. Morokuma, D. K. Malick, A. D. Rabuck, K. Raghavachari, J. B. Foresman, J. Cioslowski, J. V. Ortiz, B. B. Stefanov, G. Liu, A. Liashenko, P. Piskorz, I. Komaromi, R. Gomperts, R. L. Martin, D. J. Fox, T. Keith, M. A. Al-Laham, C. Y. Peng, A. Nanayakkara, C. Gonzalez, M. Challacombe, P. M. W. Gill, B. G. Johnson, W. Chen, M. W. Wong, J. L. Andres, M. Head-Gordon, E. S. Replogle and J. A. Pople, GAUSSIAN 98 (Revision A.6), Gaussian, Inc., Pittsburgh, PA, 1998.
19 W. J. Hehre, L. Radom, P. v. R. Schleyer and J. A. Pople, *Ab initio Molecular Orbital Theory*, Wiley, New York, 1986.
20 H. B. Schlegel, *Geometry Optimization on Potential Energy Surfaces, in Modern Electronic Structure Theory*, ed. D. R. Yarkony, World Scientific Publishing: Singapore, Singapore, 1994.
21 K. Fukui, *J. Phys. Chem.*, 1970, **74**, 4161–4163.
22 (*a*) C. González and H. B. Schlegel, *J. Phys. Chem.*, 1990, **94**, 5523–5527; (*b*) C. González and H. B. Schlegel, *J. Chem. Phys.*, 1991, **95**, 5853–5860.
23 K. B. Wiberg, *Tetrahedron*, 1968, **24**, 1083–1096.
24 E. D. Glendening, A. E. Reed, J. E. Carpenter and F. Weinhold, NBO version 3.1 in Gaussian 98.
25 (*a*) L. E. Chirlian and M. M. Francl, *J. Comput. Chem.*, 1987, **8**, 894–905; (*b*) C. M. Breneman and K. B. Wiberg, *J. Comput. Chem.*, 1990, **11**, 361–373.
26 SPARTAN V4.0, Wavefunction, Inc., 18401 Von Karman Ave, #370, Irvine, CA 92715, 1995.
27 (*a*) O. Tapia, *J. Math. Chem.*, 1992, **10**, 139–181; (*b*) J. Tomasi and M. Persico, *Chem. Rev.*, 1994, **94**, 2027–2094; (*c*) B. Y. Simkin and I. Sheikhet, *Quantum Chemical and Statistical Theory of Solutions-A Computational Approach*, Ellis Horwood, London, 1995.
28 (*a*) M. T. Cances, V. Mennunci and J. Tomasi, *J. Chem. Phys.*, 1997, **107**, 3032–3041; (*b*) M. Cossi, V. Barone, R. Cammi and J. Tomasi, *J. Chem. Phys. Lett.*, 1996, **255**, 327–335; (*c*) V. Barone, M. Cossi and J. Tomasi, *J. Comput. Chem.*, 1998, **19**, 404–417.
29 The analysis of the Fab' ab33F12 binding site has been performed using the VMD program. W. Humphrey, A. Dalke and K. Schulten, *J. Mol. Graphics*, 1996, **14**, 33–38.
30 (*a*) S. Bahmanyar and K. N. Houk, *J. Am. Chem. Soc.*, 2001, **123**, 12911–12912; (*b*) K. N. Rankin, J. W. Gauld and R. J. Boyd, *J. Phys. Chem. A*, 2002, **106**, 5155–5159; (*c*) M. Arno and L. R. Domingo, *Theor. Chem. Acc.*, 2002, **108**, 232–239.
31 B. Golinelli-Pimpaneau, *Curr. Opin. Struct. Biol.*, 2000, **10**, 697–708.
32 PCMODEL V4.0, Serena Software, Bloomington, 1990.
33 D. J. Tantillo and K. N. Houk, *J. Org. Chem.*, 1999, **64**, 3066–3076.
34 (*a*) O. Ritzeler, S. Parel, B. Therrien, N. Bensel, J.-L. Reymond and K. Schenk, *Eur. J. Org. Chem.*, 2000, 1365–1372; (*b*) B. B. Braunheim, C. K. Bagdassarian, V. L. Schramm and S. D. Schwartz, *Int. J. Quantum Chem.*, 2000, **78**, 195–205.